European Journal of Medicinal Chemistry 67 (2013) 221–229

Contents lists available at SciVerse ScienceDirect

European Journal of Medicinal Chemistry

journal homepage: http://www.elsevier.com/locate/ejmech

Preliminary communication

An expedient, ionic liquid mediated multi-component synthesis of novel piperidone grafted cholinesterase enzymes inhibitors and their molecular modeling study

Alireza Basiri [a], Vikneswaran Murugaiyah [a,*], Hasnah Osman [b], Raju Suresh Kumar [c,**], Yalda Kia [b], Khalijah Binti Awang [d], Mohamed Ashraf Ali [e]

[a] School of Pharmaceutical Sciences, Universiti Sains Malaysia, Minden 11800, Penang, Malaysia
[b] School of Chemical Sciences, Universiti Sains Malaysia, Minden 11800, Penang, Malaysia
[c] Department of Chemistry, College of Sciences, King Saud University, PO Box 2455, Riyadh, Saudi Arabia
[d] Department of Chemistry, Faculty of Science University of Malaya, 50603 Kuala Lampur, Malaysia
[e] Institute for Research in Molecular Medicine, Universiti Sains Malaysia, Minden 11800, Penang, Malaysia

ARTICLE INFO

Article history:
Received 1 June 2013
Received in revised form
19 June 2013
Accepted 24 June 2013
Available online 4 July 2013

Keywords:
AChE
BChE
Multi-component reaction
Ionic liquid
Molecular modeling

ABSTRACT

Series of hitherto unreported piperidone grafted pyridopyrimidines synthesized through ionic liquid mediated multi-component reaction. These compounds were evaluated for their inhibitory activities against AChE and BChE enzymes. All the compounds displayed considerable potency against AChE with IC_{50} values ranging from 0.92 to 9.11 μM, therein compounds **6a**, **6h** and **6i** displayed superior enzyme inhibitory activities compared to standard drug with IC_{50} values of 0.92, 1.29 and 2.07 μM. Remarkably, all the compounds displayed higher BChE inhibitory activity compared to galantamine with IC_{50} values of 1.89–8.13 μM. Molecular modeling, performed for the most active compounds using three dimensional crystal structures of *Tc*AChE and *h*BChE, disclosed binding template of these inhibitors into the active site of their respective enzymes.

1. Introduction

According to World Alzheimer's Report 2012, there are 36 million people living with dementia worldwide, which is predicted to increase up to 115 million by 2050 unless there is a cure or treatment to delay the onset or progression of the disease [1]. Alzheimer's disease (AD) is the most common type of dementia. Biochemical deficits in AD patients arise from degeneration of the cholinergic neurons caused by the phosphorylation of tau proteins leading to development of neurofibrillary tangles and formation of β-amyloid senile plaques. This neurodegeneration leads to remarkable reduction of neurotransmitter acetylcholine at the synaptic clefts [2,3]. Since acetylcholine plays a major role in cognitive processes, increasing acetylcholine levels to restore the substantial impairment of memory and cognitive dysfunctions in AD patients, the so-called cholinergic hypothesis, has gained interest [4].

Currently approved pharmacological treatments for AD are limited to cholinesterase inhibitors (ChEI's), working by inhibiting cholinesterase enzymes from hydrolyzing acetylcholine to restore the cholinergic function as well as the *N*-methyl D-aspartate receptor antagonist (e.g. memantine), which acts at the glutaminergic pathway [5–7]. Despite the tremendous efforts in search of disease modifying agents working along with the β-amyloid or tau pathways, none are clinically available due to their adverse effects. Therefore, the search for new cholinesterase enzymes inhibitors is still ongoing worldwide.

Both cholinesterase enzymes acetylcholinesterase (AChE) and butyrylcholinesterase (BChE) are involved in the hydrolysis of acetylcholine; however studies showed that as the disease progresses, the activity of AChE decreases while the activity of BChE remains unaffected or even increases [8]. In the brain of advanced staged AD patients, BChE can compensate for AChE when the activity of AChE is inhibited by AChE inhibitors. Thus, BChE hydrolyses the already depleted levels of ACh in these patients [9,10]. It has been

* Corresponding author. Tel./fax: +6046534583.
** Corresponding author.
E-mail addresses: dr.Murugaiyah@gmail.com (V. Murugaiyah), sraju@ksu.edu.sa (R.S. Kumar).

0223-5234/$ – see front matter © 2013 Elsevier Masson SAS. All rights reserved.
http://dx.doi.org/10.1016/j.ejmech.2013.06.054

Table 1
Residue composition of active sites in *Tc*AChE and *h*BChE.

Entry	Site name	Residue composition in *Tc*AChE	Residue composition in *h*BChE [34]
1	Catalytic triad	Ser200, His440 and Glu327	His438, Ser198 and Glu325
2	Choline binding site (α-anionic site)	Trp84 and Phe330	Trp82 and Phe329
3	Acyl-binding pocket	Phe288 and Phe290	Leu286 and Val288
4	Oxyanion hole	Gly118, Gly117 and Ala201	Gly116, Gly117 and Ala199
5	Peripheral anionic site (β-anionic site)	Tyr 70, Asp72, Tyr 121, Trp279 and Tyr334	Trp231, Val288, Leu286 and Phe398

also proposed that individuals with low-activity of BChE can sustain cognitive functions better comparing to individuals with normal BChE activity [11]. Furthermore, restoration of ACh levels by BChE inhibition seems to occur without apparent adverse effects [9].

Molecular modeling plays an important role in the rational drug design and is used to predict the bonding affinity, spatial orientation and total binding energy of the small molecule drug candidates to the active site of their target enzymes [12]. Active site of AChE and BChE enzymes is located deep in the center of the molecule with a narrow gorge made up of five important regions to accommodate and hydrolyze the acetylcholine substrate, namely, catalytic triad [13], oxyanion hole [14], choline binding site [15], acyl binding pocket [16] and peripheral anionic site (Table 1) [17]. In AChE, aromatic residues such as tryptophan (Trp) and phenylalanine (Phe) comprise the active site gorge, whilst in BChE the gorge is lined with hydrophobic residues such as valine (Val), which allows accommodation of bulkier substrates [17].

In the context of green chemistry, ionic liquid (IL) mediated multicomponent reactions gained much attentions as an efficient synthetic tool from the viewpoint of evasion from intermediate isolation and purification steps, effectively merged with unique properties of green ionic solvents such as strong solvating ability, catalytic behavior and recyclability [18,19]

Natural and synthetic biologically active compounds with pyrimidine moiety, find wide applications in pharmaceutical field [20] as antihypertensive [21], α_1-adrenergic receptor antagonist [22], antibacterial, anti-inflammatory, antitumor [23] and anti-HIV agents [24–26]. Moreover, compounds comprising thiourea and pyrimidine entities are reported to possess potent dual cholinesterase and Aβ-aggregation inhibitory properties [27–31]. Inspired by the aforementioned inhibitory potential of pyrimidine derivatives on cholinesterase enzymes activity and in search of new potent AChE/BChE enzymes inhibitors, in the present study we report an efficient method to synthesize biologically active piperidone grafted pyridopyrimidines *via* microwave assisted, multicomponent reaction methodology in ionic liquid and their cholinesterase enzyme inhibitory activities.

2. Result and discussion

2.1. Chemistry

N-Substituted piperidine-4-ones **2**/**3** were prepared by refluxing 4-piperidone monohydrate hydrochloride (**1**) and ethyl bromide (**2**)/4-(2-chloroethyl)morpholine (**3**) in ethanol (Scheme 1). With the functionalized piperidones **2**/**3** in hand, the aim is to synthesize pyridopyrimidine-2-thiones using ionic liquid as green solvent. To optimize the reaction conditions, initially a model reaction of 1-ethylpiperidine-4-one, benzaldehyde and thiourea in 1:2:1 molar ratio in 1 M equiv of [BMIM]Br was performed under conventional heating, the reaction progress was monitored by TLC. After completion of the reaction (60 min), the product was isolated (52%) through flash column chromatography. Subsequently, the same reaction was investigated also, under microwave irradiation which as in the case of thermal reaction, the reactants in 1 M equiv of [BMIM]Br was subjected to microwave irradiation. After completion of the reaction (2 min), the pyridopyrimidine-2-thiones were isolated as the single reaction product through column chromatography in 71% yield. The above results clearly showed that microwave irradiation led to an enhancement in the yield of the product and the reaction time has also been reduced over the conventional thermal method. Consequently, all other reactions were performed under microwave irradiation.

The structure of the pyridopyrimidine-2-thiones **6**/**7** is in accordance with the combustion data, 1D and 2D NMR spectroscopic data and IR spectroscopy (*vide infra*). In the ^{1}H NMR spectrum of **7c**, the singlet at 5.58 ppm is readily assigned to H-4, which shows HMBC correlations with the doublets at 2.90 and 3.18 ppm (J = 16.75 Hz) enabling their assignment to H-5a and H-5b. A doublet and a multiplet at 3.40 (J = 13.60 Hz) and 3.52–3.54 ppm

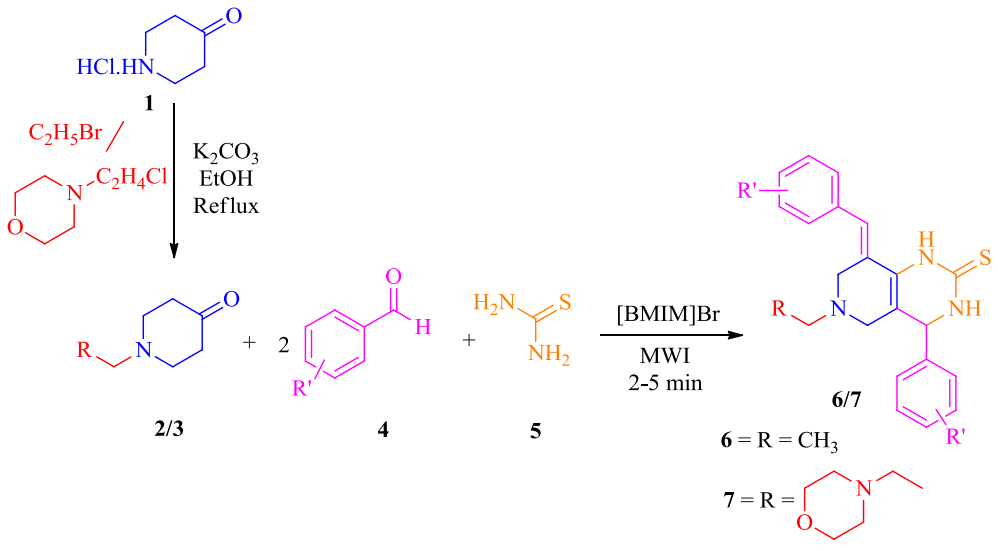

Scheme 1. Synthesis of **6**(**a**–**j**) and **7**(**a**–**j**).

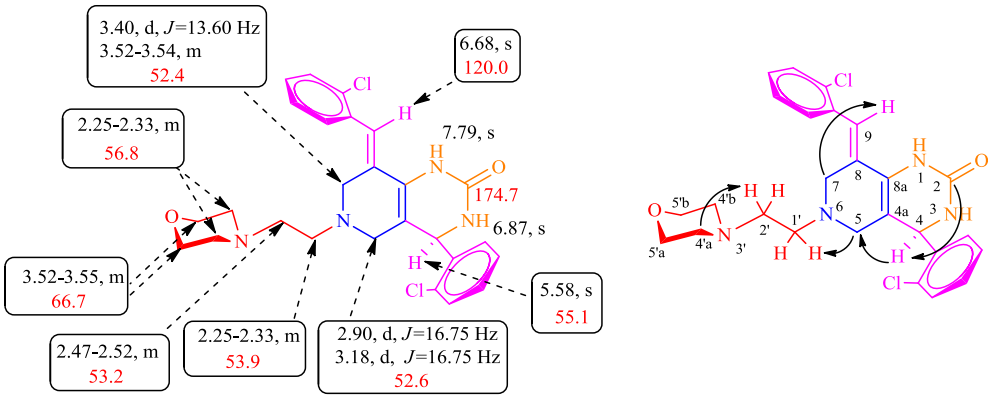

Fig. 1. Selected HMBC correlations and ^{1}H and ^{13}C chemical shifts of **7c**.

can be assigned to H-7a and H-7b. From the HMBC correlations of C-7, the multiplet around 2.25–2.33 ppm is assigned to CH_2-1′ while the other multiplet around 2.47–2.52 ppm is due to CH_2-2′. The morpholine ring hydrogens appeared as multiplets at 2.25–2.33 ppm and 3.52–3.55 ppm. A hydrogen singlet at 6.68 ppm is due to H-9 and two singlets at 6.87 and 7.79 ppm are due to two NH while the aromatic hydrogens appear as multiplets in the region 7.14–7.47 ppm. The assignment of carbon signals bearing hydrogens has been done from the chemical shifts of hydrogens and C,H-COSY correlations. These assignments are also supported by the HMBC correlations (Fig. 1) of **7c**. In addition, the structure and stereochemistry of the pyridopyrimidine-2-thiones were confirmed by the single crystal X-ray crystallographic analysis of **7b** (Fig. 2) [32]. The probable mechanism for the formation pyridopyrimidine-2-thiones (**6**/**7**) in [BMIM]Br *via* Michael addition–condensation–tautomerization domino sequence is shown in Scheme 2.

2.2. AChE and BChE inhibitory assay

All the newly synthesized compounds were evaluated for their cholinesterase inhibitory activities against AChE enzyme derived from *electric eel* and BChE enzyme from equine serum. As summarized in Table 2, both series displayed remarkable AChE and BChE inhibitory activities with IC_{50} values of lower than 10 μM. Among the newly synthesized compounds, phenyl un-substituted derivative **6a**, displayed significant sub-micromolar AChE inhibitory activity with IC_{50} value of 0.92 μM while *ortho*-methyl substituted derivative **7b**, showed highest BChE inhibitory activity with IC_{50} value of 1.89 μM. Generally, all *N*-ethyl substituted in series **6** except for *ortho*-chloroderivative, displayed better AChE inhibitory activity compared to their *N*-ethylmorpholino substituted analogs in series **7**.

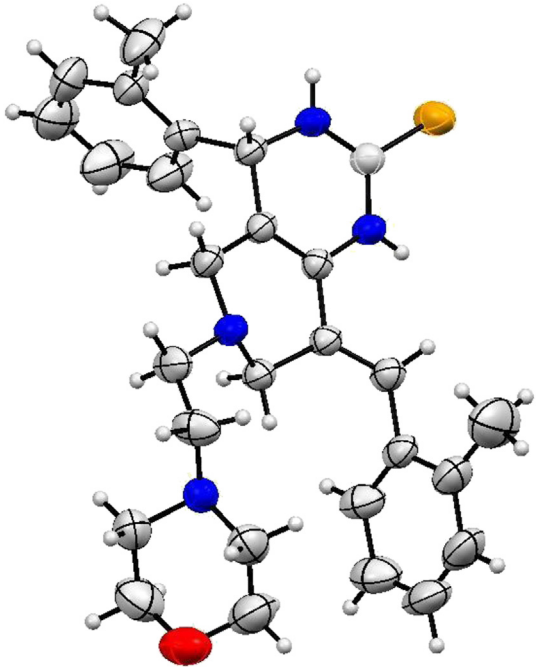

Fig. 2. ORTEP diagram of **7b**.

In both series, *para* substituted derivatives displayed better AChE inhibitory activities compared to their *ortho* substituted analogs. It is worth to note that un-substituted derivatives **6a** and **7a** possessed the highest AChE inhibitory potentials among their respective series followed by *para*-chloro and *para*-fluoro derivatives. These results clearly indicate that presence of electronegative atoms at *para* position of phenyl ring *viz.* chloro and fluoro have noticeable influence on AChE inhibitory activities observed. However, di-chloro derivatives, **6j** and **7j** displayed lower AChE enzyme inhibitory compared to mono-chloro derivatives in both series. Besides, compounds possessing electron donating moieties such as $-CH_3$ and $-OCH_3$ displayed lower AChE inhibitory activities than the electron withdrawing moieties. To compare the AChE inhibitory activities to standard drug, un-substituted **6a** (IC_{50} = 0.92 μM), *para*-chloro substituted **6h** (IC_{50} = 1.29 μM) and *para*-fluoro substituted derivative **6i** (IC_{50} = 2.07 μM) displayed higher AChE inhibitory activities than galantamine with IC_{50} value of 2.09 μM.

For BChE, compounds in series **7** displayed up to two fold higher enzyme inhibitory activity compared to compounds in series **6**, except for **7f** and **7j**. In contrary to AChE, *ortho*-substituted derivatives in series **6** and **7** displayed better BChE inhibitory activity compared to their *para*-substituted analogs. Interestingly, all newly synthesized compounds possessing either electron withdrawing or electron donating substituents on phenyl ring displayed remarkable BChE inhibitory activities with IC_{50} values of 1.89–8.13 μM that is much higher than galantamine with IC_{50} value of 19.34 μM. It is also worth to note that except for **6a**, **6e**, **6h** and **6i**, all the compounds displayed 1.2–4.31 times more selectivity toward BChE rather than AChE. As mentioned in the Introduction section, inhibitors with good balance between AChE and BChE inhibition such as **6a**, **6h** and **6i** or more selective toward BChE such as **7b**, are valuable therapeutic targets in AD therapy.

2.3. Molecular modeling

Molecular modeling simulation performed for the most potent AChE and BChE inhibitors, **6a** and **7b**, to disclose their binding

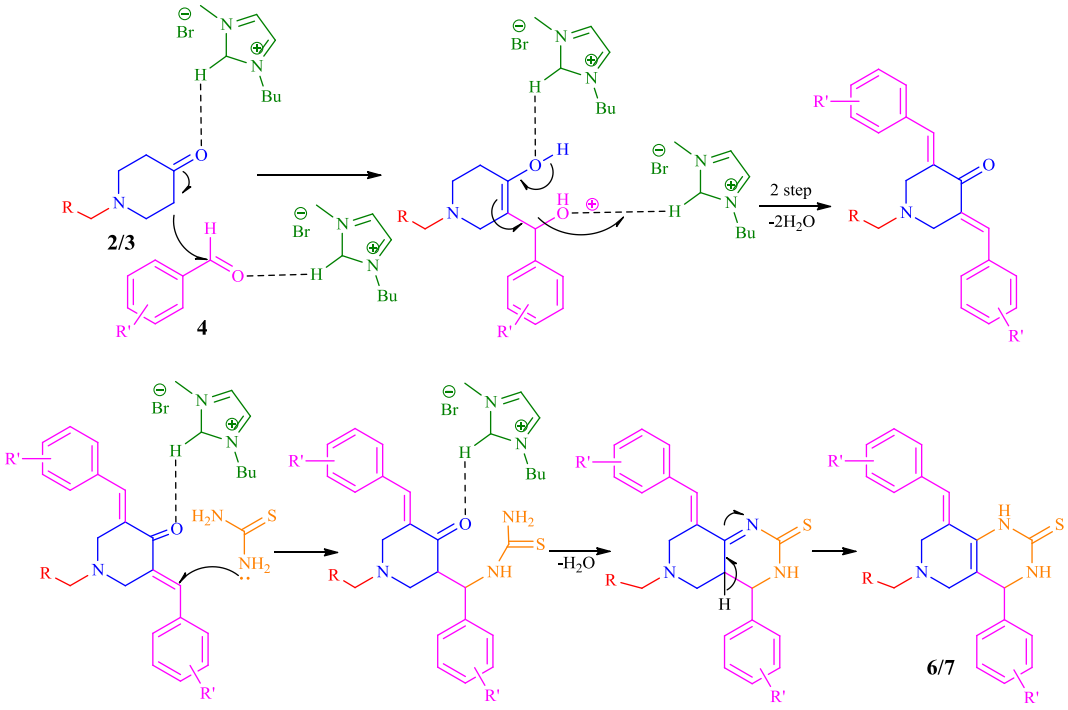

Scheme 2. Plausible mechanism for the formation of novel pyridopyrimidine-2-thiones **6**/**7**.

interactions and orientation template inside the active site gorge of their respective enzymes, by using three dimensional crystal structures of *Torpedo californa* AChE and human BChE. As depicted in Fig. 3, compound **6a**, is completely accommodated inside the active site gorge of *Tc*AChE displaying mild polar interaction with Ser200 and His440 at catalytic triad of this enzyme. At choline binding site, it is stacked against Trp84 while simultaneously showing hydrophobic interaction with Tyr334 residue. Compound **6a** also showed mild polar interactions with Gly117 and Gly118 at oxyanion hole, hydrophobic interactions with Phe288 and Phe290 at acyl binding pocket as well as hydrophobic interactions with Trp279, Tyr121, Tyr334 and Phe331 residues comprising the entrance of the gorge at peripheral anionic site. Based on this binding interaction template, this inhibitor completely fills in the gorge and prohibits substrate accommodation and hydrolysis in the active site of the enzyme, which coincides with the significant sub micromolar AChE inhibitory activity observed for this compound. Moreover, the crystal structures of *Tc*AChE enzyme in complex with

Table 2
Physical data, *Ee*AChE and *Eq*BChE activities of **6**(**a**–**j**) and **7**(**a**–**j**).

Entry	Compound	R′	Yield[a] (%)	Reaction time (min) MWI	AChE inhibition (IC_{50}) (μM)	BChE inhibition (IC_{50}) (μM)	Selectivity	
							AChE[b]	BChE[c]
1	**6a**	H	71	2	0.92	4.20	4.56	0.22
2	**6b**	2-CH_3	63	2.5	6.17	3.93	0.64	1.57
3	**6c**	2-Cl	65	2.5	8.22	3.57	0.43	2.30
4	**6d**	2-F	62	2.5	5.54	4.48	0.81	1.24
5	**6e**	2-OCH_3	73	<2	4.92	8.13	1.65	0.61
6	**6f**	3-NO_2	63	4	7.88	5.11	0.65	1.54
7	**6g**	4-CH_3	70	<2	5.02	4.73	0.94	1.06
8	**6h**	4-Cl	68	<2	1.29	5.88	4.56	0.22
9	**6i**	4-F	64	<2	2.07	5.98	2.76	0.36
10	**6j**	2,4-Cl_2	61	5	8.75	3.61	0.41	2.42
11	**7a**	H	69	3	4.49	3.23	0.72	1.39
12	**7b**	2-CH_3	67	3.5	8.15	1.89	0.23	4.31
13	**7c**	2-Cl	63	4	6.75	2.44	0.36	2.77
14	**7d**	2-F	68	4	9.32	2.97	0.32	3.14
15	**7e**	2-OCH_3	74	2	8.39	5.93	0.71	1.42
16	**7f**	3-NO_2	58	5	9.11	5.16	0.57	1.77
17	**7g**	4-CH_3	72	3	7.16	3.58	0.50	2.00
18	**7h**	4-Cl	71	3	5.49	4.28	0.78	1.28
19	**7i**	4-F	69	5	6.72	3.41	0.51	1.97
20	**7j**	2,4-Cl_2	62	5	8.67	5.87	0.68	1.47
21	–	Galantamine	–	–	2.09	19.34	9.25	0.11

[a] Isolated yield after purification by column chromatography.
[b] Selectivity for AChE is defined as IC_{50}(BChE)/IC_{50}(AChE).
[c] Selectivity for BChE is defined as IC_{50}(AChE)/IC_{50}(BChE).

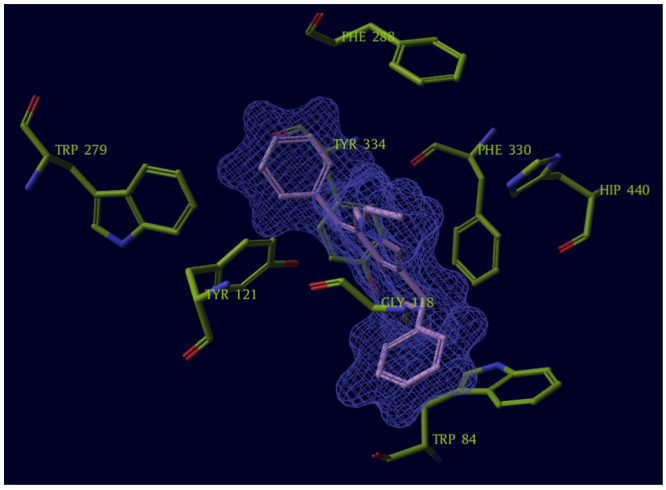

Fig. 3. Binding interactions of **6a** with major active site residues of *Tc*AChE receptor.

available Alzheimer's drugs such as huperzine A, galantamine and donepezil also show similar interactions of occupying the peripheral anionic site, stacking against Trp84 and interacting with residues at catalytic triad [33]

Molecular docking analysis of **7b** into the active site of *h*BChE also displayed the complete insertion and efficient accommodation of this inhibitor into the active site gorge of the enzyme by displaying π,π-stacking interaction with choline binding site residue, Trp82 and mild polar interaction with catalytic triad residues, His438 and Ser198, at the bottom of the gorge. This molecule also showed mild polar interactions with Gly116 and Gly117 at oxyanion hole in addition to hydrophobic interactions with Trp231, Leu286 comprising peripheral anionic site and Phe398 and Ala199 composing acyl binding pocket of the *h*BChE active site (Fig. 4). This binding interaction template also, resembles the reported template for *h*BChE receptor in complex with its substrate, butyrylcholine, which obviously coincides with potent *in vitro* BChE inhibitory activity observed for this compound [34]. The data representing free binding energies, receptors interacting sites, ligand interacting moieties, amino acid residues involved in ligand–receptor complex as well as their bonding types regarding compounds **6a** and **7b** are summarized in Table 3.

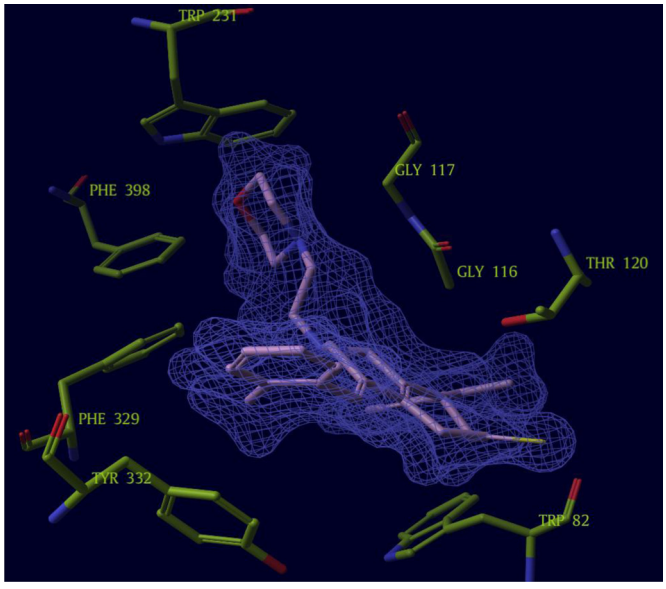

Fig. 4. Binding interactions of **7b** with major active site residues of *h*BChE receptor.

3. Conclusion

Two series of novel piperidone grafted pyrimidine derivatives as potential cholinesterase inhibitor agents have been synthesized *via* an ionic liquid mediated multi-component reaction of *N*-substituted 4-piperidones, aromatic aldehydes and thiourea under microwave irradiation. The synthesized compounds were found to be potent against both AChE and BChE enzymes with significant IC_{50} values of less than 10 μM as compared to standard drug. Further structural modification to improve their cholinesterase enzyme inhibitory potency is being carried out in our laboratory.

4. Experimental

4.1. Chemistry

The chemicals used were obtained from Merck (Germany) and Sigma Aldrich (USA). Melting points were determined by open tube capillary method and are uncorrected. Purity of the compounds was checked on thin layer chromatography (TLC) plates (silica gel G) using the petroleum ether/ethyl acetate solvent system and the spots were examined under UV light. IR spectra were obtained on a Perkin–Elmer 1720 FT-IR spectrometer (KBr Pellets). ^{1}H and ^{13}C NMR were performed on Bruker Avance 500 (^{1}H: 500 MHz, ^{13}C: 125 MHz) spectrometer in $CDCl_3$, using TMS as internal standard. Mass spectra were recorded on Varian 320-MS TQ LC/MS using ESI.

4.1.1. General procedure for synthesis of (*6a–j*) and (*7a–j*)

1 M equiv of [BMIM]Br was added to 1:2:1 ratio of 1-ethylpiperidine-4-one (**2**)/1-(morpholinoethyl)piperidine-4-one (**3**), aromatic aldehydes (**4**) and thiourea (**5**). The mixture mixed well and irradiated for 2–5 min at maximum power level (300 W) in a CEM microwave synthesizer during which period till completion of reaction as evident by TLC. Subsequently, mixture purified using flash column chromatography to afford compounds **6a–j** and **7a–j** in good yields (Table 2).

*4.1.1.1. (E)-8-Benzylidene-6-ethyl-4-phenyloctahydropyrido[4,3-d] pyrimidine-2(1H)-thione (**6a**).* Yellow solid; mp 164–167 °C; IR (KBr) ν_{max}: 2973, 1542, 1487 cm^{-1}. Anal. calcd. for $C_{22}H_{25}N_3S$: C, 72.69; H, 6.93; N, 11.56. Found: C, 72.12; H, 7.21; N, 10.94. ^{1}H NMR (500 MHz, $CDCl_3$): δ_H 0.92–0.96 (m, 3H, CH_3), 2.38–2.42 (m, 2H, CH_2), 2.67 (d, 1H, J = 16.07 Hz, H-5a), 3.07 (d, 1H, J = 16.07 Hz, H-5b), 3.30 (d, 1H, J = 13.55 Hz, H-7a), 3.63 (d, 1H, J = 13.55 Hz, H-7b), 5.01 (s, 1H, H-4), 6.64 (s, 1H, H-9), 7.20–7.36 (m, 12H, H-aromatic, NH). ^{13}C NMR (125 MHz, $CDCl_3$): δ_C 11.84, 50.73, 51.64, 51.72, 59.12, 110.79, 123.11, 125.66, 127.20, 127.53, 128.40, 128.85, 129.14, 129.52, 130.37, 135.64, 140.83, 173.52.

*4.1.1.2. (E)-6-Ethyl-8-(2-methylbenzylidene)-4-(o-tolyl)octahydropyrido[4,3-d]pyrimidine-2(1H)-thione (**6b**).* Yellow solid; mp 160–162 °C; IR (KBr) ν_{max}: 2974, 1546, 1489 cm^{-1}. Anal. calcd. for $C_{24}H_{29}N_3S$: C, 73.62; H, 7.46; N, 10.73. Found: C, 72.92; H, 7.05; N, 10.19. ^{1}H NMR (500 MHz, $CDCl_3$): δ_H 0.99–1.04 (m, 3H, CH_3), 2.26–2.40 (m, 5H, CH_2 and CH_3), 2.76 (d, 1H, J = 16.15 Hz, H-5a), 3.04 (d, 1H, J = 16.15 Hz, H-5b), 3.26 (d, 1H, J = 13.47 Hz, H-7a), 3.65 (d, 1H, J = 13.47 Hz, H-7b), 4.97 (s, 1H, H-4), 6.61 (s, 1H, H-9), 7.08–7.21 (m, 10H, H-aromatic, NH). ^{13}C NMR (125 MHz, $CDCl_3$): δ_C 12.18, 21.18, 21.21, 21.27, 48.77, 50.99, 51.27, 51.46, 59.20, 106.20, 122.38, 125.84, 127.17, 127.23, 129.14, 129.21, 129.68, 129.80, 132.82, 137.45, 138.20, 138.56, 138.76, 173.92.

Table 3
Binding Interaction data for **6a** and **7b** docked into active site gorge of *Tc*AChE and *h*BChE receptors.

Entry	Ligand	Enzyme	Binding energy (kcal)	Interacting site	Amino acid residue	Bond type	Ligand interacting moiety
1	**6a**	*Tc*AChE	−8.0	PAS[a]	Trp279	Hydrophobic	Ring 1
					Tyr334	Hydrophobic	
					Asp72	Mild polar	Ring 2
					Tyr121	Hydrophobic	N-ethyl
				OH[b]	Gly117 and 118	Mild polar	Ring 4
				Acyl binding pocket	Phe288	Hydrophobic	Ring 3
					Phe290	Hydrophobic	
				Choline binding site	Phe330	Hydrophobic	Ring 2
					Trp84	Hydrophobic	Ring 4
				CT[c]	Ser200	Mild polar	Ring 4
					His 440	Mild polar	
2	**7b**	*h*BChE	−7.7	Side chain	Pro285	Hydrophobic	Ring 1
					Ser287	Mild polar	
					Thr120	Mild polar	Ring 4
				PAS	Tyr332	Hydrophobic	Ring 1
					Leu286	Hydrophobic	Morpholine moiety
					Val288	Hydrophobic	
				OH	Gly116 and 117	Mild polar	Ring 4
				Choline binding site	Phe329	Hydrophobic	Morpholine moiety
					Trp82	π–π stacking	Ring 4
				CT	His438	Mild polar	Morpholine moiety
					Ser198	Mild polar	Morpholine moiety

[a] Peripheral anionic site.
[b] Oxyanion hole.
[c] Catalytic triad.

*4.1.1.3. (E)-8-(2-Chlorobenzylidene)-4-(2-chlorophenyl)-6-ethyloctahydropyrido[4,3-d]pyrimidine-2(1H)-thione (**6c**).* Yellow solid; mp 137–139 °C; IR (KBr) ν_{max}: 2971, 1547, 1488 cm^{-1}. Anal. calcd. for $C_{22}H_{23}Cl_2N_3S$: C, 61.11; H, 5.36, N, 9.72. Found: C, 62.12; H, 5.07, N, 8.94. ^1H NMR (500 MHz, $CDCl_3$): δ_H 0.87–0.95 (m, 3H, CH_3), 2.37–2.44 (m, 2H, CH_2), 2.80 (d, 1H, J = 16.27 Hz, H-5a), 3.11 (d, 1H, J = 16.27 Hz, H-5b), 3.29 (d, 1H, J = 13.39 Hz, H-7a), 3.44 (d, 1H, J = 13.39 Hz, H-7b), 5.59 (s, 1H, H-4), 6.67 (s, 1H, H-9), 7.14–7.48 (m, 10H, H-aromatic, NH). ^{13}C NMR (125 MHz, $CDCl_3$): δ_C 12.09, 31.11, 50.90, 51.27, 51.71, 52.53 55.20, 110.79, 119.18, 126.47, 127.15, 127.32, 128.24, 128.67, 128.82, 129.25, 129.58, 129.76, 130.18, 131.74, 133.77, 137.26,174.60.

*4.1.1.4. (E)-6-Ethyl-8-(2-fluorobenzylidene)-4-(2-fluorophenyl)octahydropyrido[4,3-d]pyrimidine-2(1H)-thione (**6d**).* Yellow solid; mp 131–134 °C; IR (KBr) ν_{max}: 3696, 2981, 1506, 1055 cm^{-1}. Anal. calcd. for $C_{22}H_{23}F_2N_3S$: C, 66.14; H, 5.80; N, 10.52. Found: C, 67.12; H, 5.21; N, 10.07. ^1H NMR (500 MHz, $CDCl_3$): δ_H 0.78–0.98 (m, 3H, CH_3), 2.38–2.45 (m, 2H, CH_2), 2.78 (d, 1H, J = 16.23 Hz, H-5a), 3.11 (d, 1H, J = 16.23 Hz, H-5b), 3.26 (d, 1H, J = 13.55 Hz, H-7a), 3.47 (d, 1H, J = 13.55 Hz, H-7b), 5.60 (s, 1H, H-4), 6.62 (s, 1H, H-9), 6.91–7.47 (m, 10H, H-aromatic, NH). ^{13}C NMR (125 MHz, $CDCl_3$): δ_C 12.16, 50.97, 51.87, 51.90, 52.30, 108.65, 115.04, 115.06, 115.54, 115.55, 115.71, 115.73, 123.75, 123.78, 125.07, 125.09, 127.84, 128.64, 128.75, 128.85, 128.88, 129.24, 129.30, 129.49, 129.95, 130.01, 130.76, 130.78, 153.74, 159.16, 174.21.

*4.1.1.5. (E)-6-Ethyl-8-(2-methoxybenzylidene)-4-(2-methoxyphenyl) octahydropyrido[4,3-d]pyrimidine-2(1H)-thione (**6e**).* Yellow solid; mp 138–140 °C; IR (KBr) ν_{max}: 3691, 2973, 1509, 1042 cm^{-1}. Anal. calcd. for $C_{24}H_{27}N_3O_2S$: C, 68.38; H, 6.46; N, 9.97. Found: C, 67.89; H, 6.15; N, 9.52. ^1H NMR (500 MHz, $CDCl_3$): δ_H 0.93 (t, 3H, J = 7.25 Hz, CH_3), 2.35–2.43 (m, 2H, CH_2), 2.61 (d, 1H, J = 15.92 Hz, H-5a), 2.97 (d, 1H, J = 15.92 Hz, H-5b), 3.27 (d, 1H, J = 13.39 Hz, H-7a), 3.62 (d, 1H, J = 13.39 Hz, H-7b), 3.79 (s, 3H, O–CH_3), 3.80 (s, 3H, O–CH_3), 4.93 (s, 1H, H-4), 5.60 (s, 1H, H-9), 6.58 (s, 1H, NH), 6.86–7.25 (m, 9H, H-aromatic, NH). ^{13}C NMR (125 MHz, $CDCl_3$): δ_C 12.25, 51.09, 52.07, 52.18, 55.26, 55.31, 59.05, 108.80, 114.33, 121.64, 126.27, 126.95, 128.37, 130.61, 133.79, 134.35, 159.01, 159.98, 173.88.

*4.1.1.6. (E)-6-Ethyl-8-(3-nitrobenzylidene)-4-(3-nitrophenyl)octahydropyrido[4,3-d]pyrimidine-2(1H)-thione (**6f**).* Yellow solid; mp 158–161 °C; IR (KBr) ν_{max}: 2969, 1542, 1457, 779 cm^{-1}. Anal. calcd. for $C_{22}H_{23}N_5O_4S$: C, 58.26; H, 5.11; N, 15.44. Found: C, 57.45; H, 4.67; N, 15.09. ^1H NMR (500 MHz, $CDCl_3$): δ_H 0.93 (t, 3H, J = 7.25 Hz, CH_3), 2.45–2.51 (m, 2H, CH_2), 2.60 (d, 1H, J = 15.92 Hz, H-5a), 3.04 (d, 1H, J = 15.92 Hz, H-5b), 3.17 (d, 1H, J = 13.55 Hz, H-7a), 3.49 (d, 1H, J = 13.39 Hz, H-7b), 5.39 (s, 1H, H-4), 5.85 (s, 1H, H-9), 7.16–8.21 (m, 10H, H-aromatic, NH). ^{13}C NMR (125 MHz, $CDCl_3$): δ_C 12.07, 50.97, 52.34, 52.53, 54.45, 109.45, 119.91, 121.64, 126.49, 126.89, 128.40, 130.81, 134.93, 158.71, 159.12, 174.42.

*4.1.1.7. (E)-6-ethyl-8-(4-methylbenzylidene)-4-(p-tolyl)octahydropyrido[4,3-d]pyrimidine-2(1H)-thione (**6g**).* Yellow solid; mp 164–166 °C; IR (KBr) ν_{max}: 2967, 1552, 1467 cm^{-1}. Anal. calcd. for $C_{24}H_{29}N_3S$: C, 73.62; H, 7.46; N, 10.73. Found: C, 72.77; H, 7.12; N, 10.27. ^1H NMR (500 MHz, $CDCl_3$): δ_H 0.92 (t, 3H, J = 7.25 Hz, CH_3), 2.32 (s, 3H, CH_3), 2.33 (s, 1H, CH_3), 2.36–2.39 (m, 2H, CH_2), 2.61 (d, 1H, J = 15.76 Hz, H-5a), 2.99 (d, 1H, J = 15.76 Hz, H-5b), 3.25 (d, 1H, J = 13.55 Hz, H-7a), 3.63 (d, 1H, J = 13.55 Hz, H-7b), 4.93 (s, 1H, H-4), 5.76 (s, 1H, H-9), 6.63 (s, 1H, NH), 6.84–7.34 (m, 9H, H-aromatic, NH). ^{13}C NMR (125 MHz, $CDCl_3$): δ_C 12.24, 21.16, 21.22, 51.03, 52.11, 52.15, 59.33, 109.05, 122.10, 126.68, 126.73, 127.01, 127.07, 129.01, 129.17, 129.23, 129.65, 133.37, 137.01, 138.16, 139.22, 174.15.

*4.1.1.8. (E)-8-(4-chlorobenzylidene)-4-(4-chlorophenyl)-6-ethyloctahydropyrido[4,3-d]pyrimidine-2(1H)-thione (**6h**).* Yellow solid; mp 162–165 °C; IR (KBr) ν_{max}: 2971, 1547, 1488, 1090 cm^{-1}. Anal. calcd. for $C_{22}H_{23}Cl_2N_3S$: C, 61.11; H, 5.36, N, 9.72. Found: C, 62.22; H, 5.16, N, 8.71. ^1H NMR (500 MHz, $CDCl_3$): δ_H 0.93 (t, 3H, J = 7.09 Hz, CH_3), 2.32–2.41 (m, 2H, CH_2), 2.57 (d, 1H, J = 16.07 Hz, H-5a), 2.93 (d, 1H, J = 16.07 Hz, H-5b), 3.23 (d, 1H, J = 13.39 Hz, H-7a), 3.50 (d, 1H, J = 13.39 Hz, H-7b), 4.89 (s, 1H, H-4), 6.11 (s, 1H, H-9), 6.67 (s, 1H, NH), 7.09–7.37 (m, 9H, H-aromatic, NH). ^{13}C NMR (125 MHz, $CDCl_3$): δ_C 12.17,

51.10, 51.97, 58.79, 109.15, 127.32, 128.05, 128.33, 128.48, 129.22, 130.54, 133.07, 134.28, 134.65, 140.54, 174.79.

*4.1.1.9. (E)-6-Ethyl-8-(4-fluorobenzylidene)-4-(4-fluorophenyl)octahydropyrido[4,3-d]pyrimidine-2(1H)-thione (**6i**).* Yellow solid; mp 150–152 °C; IR (KBr) ν_{max}: 3696, 2973, 1505, 1055 cm^{-1} Anal. calcd. for $C_{22}H_{23}F_2N_3S$: C, 66.14; H, 5.80; N, 10.52. Found: C, 67.29; H, 5.34; N, 10.15. ^1H NMR (500 MHz, $CDCl_3$): δ_H 0.81–0.99 (m, 3H, CH_3), 2.35–2.44 (m, 2H, CH_2), 2.75 (d, 1H, J = 16.19 Hz, H-5a), 3.09 (d, 1H, J = 16.19 Hz, H-5b), 3.31 (d, 1H, J = 13.47 Hz, H-7a), 3.52 (d, 1H, J = 13.47 Hz, H-7b), 5.52 (s, 1H, H-4), 6.53 (s, 1H, H-9), 6.87–7.39 (m, 10H, H-aromatic, NH). ^{13}C NMR (125 MHz, $CDCl_3$): δ_C 12.12, 50.87, 51.91, 51.93, 52.13, 109.05, 115.02, 115.07, 115.49, 115.51, 115.68, 115.71, 123.89, 123.97, 125.17, 125.21, 127.77, 128.69, 128.78, 128.94, 129.12, 129.38, 129.45, 129.69, 130.07, 130.15, 130.88, 130.94, 153.72, 159.24, 175.16.

*4.1.1.10. (E)-8-(2,4-Dichlorobenzylidene)-4-(2,4-dichlorophenyl)-6-ethyloctahydropyrido[4,3-d]pyrimidine-2(1H)-thione (**6j**).* Yellow solid; mp 142–145 °C; IR (KBr) ν_{max}: 2977, 1548, 1452 cm^{-1}. Anal. calcd. for $C_{22}H_{21}Cl_4N_3S$: C, 52.71; H, 4.22; N, 8.38. Found: C, 52.34; H, 3.99; N, 8.12. ^1H NMR (500 MHz, $CDCl_3$): δ_H 0.95 (t, 3H, J = 7.25 Hz, CH_3), 2.38–2.44 (m, 2H, CH_2), 2.78 (d, 1H, J = 16.07 Hz, H-5a), 3.11 (d, 1H, J = 16.07 Hz, H-5b), 3.30 (d, 1H, J = 13.71 Hz, H-7a), 3.44 (d, 1H, J = 13.71 Hz, H-7b), 4.78 (s, 1H, H-4), 5.55 (s, 1H, H-9), 6.65 (s, 1H, NH), 7.17–7.50 (m, 7H, H-aromatic, NH). ^{13}C NMR (125 MHz, $CDCl_3$): δ_C 12.14, 51.00, 51.93, 52.14, 55.14, 109.05, 126.33, 128.04, 128.11, 128.84, 129.32, 129.62, 129.88, 130.65, 132.72, 134.26, 138.53, 174.61.

*4.1.1.11. (E)-8-Benzylidene-6-(2-morpholinoethyl)-4-phenyloctahydropyrido[4,3-d]pyrimidine-2(1H)-thione (**7a**).* Yellow solid; mp 110–112 °C; IR (KBr) ν_{max}: 3185, 2967, 1543, 1454 cm^{-1}. Anal. calcd. for $C_{26}H_{32}N_4OS$: C, 69.61; H, 7.19; N, 12.49. Found: C, 69.17; H, 6.78; N, 12.18. ^1H NMR (500 MHz, $CDCl_3$): δ_H 2.21–2.31 (m, 6H, CH_2-1′, CH_2-4′), 2.44–2.49 (m, 2H, CH_2-2′), 2.91 (d, J = 16.55 Hz, H-5a), 3.21 (d, J = 16.55 Hz, H-5b), 3.38 (d, J = 13.72 Hz, H-7a), 3.49–3.54 (m, 5H, H-7b, CH_2-5′), 5.41 (s, 1H, H-4), 6.65 (s, 1H, H-9), 6.85 (s, 1H, NH), 7.81 (s, 1H, NH), 7.24–7.39 (m, 10H, H-aromatic). ^{13}C NMR (125 MHz, $CDCl_3$): δ_C 52.37, 52.54, 53.17, 53.82, 55.09, 56.78, 66.71, 109.98, 119.17, 125.44, 126.91, 127.45, 128.32, 128.92, 129.34, 130.12, 130.34, 130.72, 132.84, 134.12, 134.29, 137.48, 174.69.

*4.1.1.12. (E)-8-(2-Methylbenzylidene)-6-(2-morpholinoethyl)-4-(o-tolyl)octahydropyrido[4,3-d]pyrimidine-2(1H)-thione (**7b**).* Yellow solid; mp 120–122 °C; IR (KBr) ν_{max}: 3178, 2958, 1551, 1033 cm^{-1}. Anal. calcd. for $C_{28}H_{36}N_4OS$: C, 70.55; H, 7.61; N, 11.75. Found: C, 70.12; H, 7.21; N, 11.09. ^1H NMR (500 MHz, $CDCl_3$): δ_H 2.24–2.34 (m, 6H, CH_2-1′, CH_2-4′), 2.35 (s, 3H, CH_3), 2.37 (s, 3H, CH_3), 2.44–2.52 (m, 2H, CH_2-2′), 2.78 (d, J = 16.21 Hz, H-5a), 3.09 (d, J = 16.21 Hz, H-5b), 3.42 (d, J = 13.54 Hz, H-7a), 3.55–3.63 (m, 4H, CH_2-5′), 3.73 (d, 1H, J = 13.54, H-7b), 4.94 (s, 1H, H-4), 6.74 (s, 1H, H-9), 7.11 (s, 1H, NH), 7.16-7.24 (m, 8H, H-aromatic), 7.79 (s, 1H, NH). ^{13}C NMR (125 MHz, $CDCl_3$): δ_C 21.02, 21.10, 52.42, 52.93, 53.67, 56.37, 58.74, 66.54, 110.20, 123.16, 125.03, 125.50, 127.06, 129.10, 129.72, 132.71, 137.53, 137.95, 138.69, 173.45.

*4.1.1.13. (E)-8-(2-Chlorobenzylidene)-4-(2-chlorophenyl)-6-(2-morpholinoethyl)octahydropyrido[4,3-d]pyrimidine-2(1H)-thione (**7c**).* Yellow solid; mp 130–132 °C; IR (KBr) ν_{max}: 2974, 1548, 1478, 1092 cm^{-1}. Anal. calcd. for $C_{26}H_{30}Cl_2N_4OS$: C, 60.34; H, 13.70; N, 10.83. Found: C, 60.11; H, 13.24; N, 10.52. ^1H NMR (500 MHz, $CDCl_3$): δ_H 2.25–2.33 (m, 6H, CH_2-1′, CH_2-4′), 2.47–2.52 (m, 2H, CH_2-2′), 2.90 (d, J = 16.75 Hz, H-5a), 3.18 (d, J = 16.75 Hz, H-5b), 3.40 (d, J = 13.60 Hz, H-7a), 3.52–3.55 (m, 5H, H-7b, CH_2-5′), 5.58 (s, 1H, H-4), 6.68 (s, 1H, H-9), 6.87 (s, 1H, NH), 7.11-7.21 (m, 8H, H-aromatic), 7.79 (s, 1H, NH). ^{13}C NMR (125 MHz, $CDCl_3$): δ_C 52.49, 52.62, 53.24, 53.90, 55.13, 56.82, 66.76, 110.50, 120.07, 126.51, 127.58, 128.25, 129.23, 129.58, 129.79, 130.04, 130.23, 130.69, 132.71, 133.78, 134.18, 137.30, 174.78.

*4.1.1.14. (E)-8-(2-Fluorobenzylidene)-4-(2-fluorophenyl)-6-(2-morpholinoethyl)octahydropyrido[4,3-d]pyrimidine-2(1H)-thione (**7d**).* Yellow solid; mp 112–115 °C; IR (KBr) ν_{max}: 3695, 2981, 1517, 1055 cm^{-1}. Anal. calcd. for $C_{26}H_{30}F_2N_4OS$: C, 64.44; H, 6.24; N, 11.56. Found: C, 64.12; H, 5.91; N, 11.19. ^1H NMR (500 MHz, $CDCl_3$): δ_H 2.15–2.37 (m, 6H, CH_2-1′, CH_2-4′), 2.36–2.43 (m, 2H, CH_2-2′), 2.67 (d, J = 16.07 Hz, H-5a), 3.01 (d, J = 16.07 Hz, H-5b), 3.34 (d, J = 13.55 Hz, H-7a), 3.43–3.51 (m, 4H, CH_2-5′), 3.63 (d, 1H, J = 13.55 Hz, H-7b), 5.49 (s, 1H, H-4), 6.60 (s, 1H, H-9), 6.75 (s, 1H, NH), 7.12 (s, 1H, NH), 7.15-7.32 (m, 8H, H-aromatic). ^{13}C NMR (125 MHz, $CDCl_3$): δ_C 51.68, 51.78, 52.41, 52.86, 55.88, 58.56, 65.74, 107.86, 121.44, 125.89, 126.13, 126.27, 127.30, 127.50, 128.03, 128.25, 135.09, 141.03, 173.99.

*4.1.1.15. (E)-8-(2-Methoxybenzylidene)-4-(2-methoxyphenyl)-6-(2-morpholinoethyl)octahydropyrido[4,3-d]pyrimidine-2(1H)-thione (**7e**).* Yellow solid; mp 108–110 °C; IR (KBr) ν_{max}: 3699, 2923, 1544, 1035 cm^{-1}. Anal. calcd. for $C_{28}H_{36}N_4O_3S$: C, 66.11; H, 7.13; N, 11.01. Found: C, 65.43; H, 6.82; N, 10.75. ^1H NMR (500 MHz, $CDCl_3$): δ_H 2.23–2.36 (m, 6H, CH_2-1′, CH_2-4′), 2.44–2.53 (m, 2H, CH_2-2′), 2.75 (d, J = 16.25 Hz, H-5a), 3.07 (d, J = 16.25 Hz, H-5b), 3.43 (d, J = 13.47 Hz, H-7a), 3.53–3.61 (m, 4H, CH_2-5′), 3.72 (d, J = 13.47 Hz, 1H, H-7b), 3.81 (s, 3H, O–CH_3), 3.83 (s, 3H, O–CH_3), 4.96 (s, 1H, H-4), 6.56 (s, 1H, H-9), 6.89 (s, 1H, NH), 6.91 (s, 1H, NH), 7.11-7.28 (m, 8H, H-aromatic). ^{13}C NMR (125 MHz, $CDCl_3$): δ_C 52.61, 52.68, 53.91, 55.34, 55.39, 56.87, 59.00, 66.79, 113.95, 114.55, 128.58, 130.66, 132.79, 160.07.

*4.1.1.16. (E)-6-(2-Morpholinoethyl)-8-(3-nitrobenzylidene)-4-(3-nitrophenyl)octahydropyrido[4,3-d]pyrimidine-2(1H)-thione (**7f**).* Yellow solid; mp 182–184 °C; IR (KBr) ν_{max}: 2967, 1542, 1454, 1035 cm^{-1}. Anal. calcd. for $C_{26}H_{30}N_6O_5S$: C, 57.98; H, 5.61; N, 15.60. Found: C, 57.25; H, 5.39; N, 15.12. ^1H NMR (500 MHz, $CDCl_3$): δ_H 2.21–2.31 (m, 6H, CH_2-1′, CH_2-4′), 2.53–2.61 (m, 2H, CH_2-2′), 2.97 (d, J = 16.49 Hz, H-5a), 3.21 (d, J = 16.49 Hz, H-5b), 3.38 (d, J = 13.72 Hz, H-7a), 3.44–3.59 (m, 5H, H-7b, CH_2-5′), 5.61 (s, 1H, H-4), 6.59 (s, 1H, H-9), 6.91 (s, 1H, NH), 7.19 (s, 1H, NH), 7.25-7.39 (m, 8H, H-aromatic). ^{13}C NMR (125 MHz, $CDCl_3$): δ_C 52.11, 52.29, 52.91, 53.28, 54.49, 56.36, 66.72, 111.09, 121.18, 127.03, 127.43, 128.11, 129.09, 129.44, 129.79, 130.12, 130.27, 130.71, 133.12, 133.69, 134.07, 140.29, 176.12.

*4.1.1.17. (E)-8-(4-Methylbenzylidene)-6-(2-morpholinoethyl)-4-(p-tolyl)octahydropyrido[4,3-d]pyrimidine-2(1H)-thione (**7g**).* Yellow solid; mp 158–160 °C; IR (KBr) ν_{max}: 3185, 2965, 1551, 1464 cm^{-1}. Anal. calcd. for $C_{28}H_{36}N_4OS$: C, 70.55; H, 7.61; N, 11.75. Found: C, 70.21; H, 7.29; N, 11.17. ^1H NMR (500 MHz, $CDCl_3$): δ_H 2.21–2.33 (m, 6H, CH_2-1′, CH_2-4′), 2.34 (s, 3H, CH_3), 2.38 (s, 3H, CH_3), 2.41–2.49 (m, 2H, CH_2-2′), 2.69 (d, J = 16.45 Hz, H-5a), 3.02 (d, J = 16.45 Hz, H-5b), 3.37 (d, J = 13.35 Hz, H-7a), 3.49–3.58 (m, 4H, CH_2-5′), 3.69 (d, 1H, J = 13.35, H-7b), 4.87 (s, 1H, H-4), 6.62 (s, 1H, H-9), 7.07 (s, 1H, NH), 7.12–7.21 (m, 8H, H-aromatic), 7.54 (s, 1H, NH). ^{13}C NMR (125 MHz, $CDCl_3$): δ_C 21.02, 21.10, 52.42, 52.93, 53.67, 56.37, 58.74, 66.54, 110.20, 123.16, 125.03, 125.50, 127.06, 129.10, 129.72, 132.71, 137.53, 137.95, 138.69, 173.45.

*4.1.1.18. (E)-8-(4-Chlorobenzylidene)-4-(4-chlorophenyl)-6-(2-morpholinoethyl)octahydropyrido[4,3-d]pyrimidine-2(1H)-thione (**7h**).* Yellow solid; mp 128–130 °C; IR (KBr) ν_{max}: 3175, 2962, 1544, 1485 cm^{-1}. Anal. calcd. for $C_{26}H_{30}Cl_2N_4OS$: C, 60.34; H, 13.70; N, 10.83. Found: C, 60.21; H, 13.12; N, 10.49. ^1H NMR (500 MHz, $CDCl_3$): δ_H

2.19–2.27 (m, 6H, CH_2-1′, CH_2-4′), 2.44–2.49 (m, 2H, CH_2-2′), 2.85 (d, J = 16.73 Hz, H-5a), 3.05 (d, J = 16.73 Hz, H-5b), 3.44 (d, J = 13.19 Hz, H-7a), 3.58–3.69 (m, 5H, H-7b, CH_2-5′), 5.67 (s, 1H, H-4), 6.71 (s, 1H, H-9), 6.97 (s, 1H, NH), 7.11-7.21 (m, 8H, H-aromatic), 7.34 (s, 1H, NH). ^{13}C NMR (125 MHz, $CDCl_3$): δ_C 52.44, 52.51, 53.23, 53.79, 55.07, 56.75, 67.01, 110.39, 121.19, 126.44, 127.67, 128.21, 129.24, 129.78, 129.45, 131.14, 131.23, 131.67, 132.11, 132.78, 133.28, 137.49, 175.17.

*4.1.1.19. (E)-8-(4-Fluorobenzylidene)-4-(4-fluorophenyl)-6-(2-morpholinoethyl)octahydropyrido[4,3-d]pyrimidine-2(1H)-thione (**7i**).* Yellow solid; mp 148–150 °C; IR (KBr) ν_{max}: 3681, 2923, 1507, 1037 cm^{-1}. Anal. calcd. for $C_{26}H_{30}F_2N_4OS$: C, 64.44; H, 6.24; N, 11.56. Found: C, 64.32; H, 5.78; N, 11.25. ^{1}H NMR (500 MHz, $CDCl_3$): δ_H 2.12–2.35 (m, 6H, CH_2-1′, CH_2-4′), 2.29–2.37 (m, 2H, CH_2-2′), 2.64 (d, J = 16.27 Hz, H-5a), 3.09 (d, J = 16.27 Hz, H-5b), 3.31 (d, J = 13.49 Hz, H-7a), 3.41–3.49 (m, 4H, CH_2-5′), 3.58 (d, 1H, J = 13.49 Hz, H-7b), 5.77 (s, 1H, H-4), 6.65 (s, 1H, H-9), 6.89 (s, 1H, NH), 7.19 (s, 1H, NH), 7.23-7.41 (m, 8H, H-aromatic). ^{13}C NMR (125 MHz, $CDCl_3$): δ_C 51.63, 51.72, 52.321, 53.11, 55.65, 58.44, 65.77, 108.19, 121.49, 125.73, 126.29, 126.48, 127.15, 127.53, 128.07, 128.35, 135.12, 144.52, 174.16.

*4.1.1.20. (E)-8-(2,4-Dichlorobenzylidene)-4-(2,4-dichlorophenyl)-6-(2-morpholinoethyl)octahydropyrido[4,3-d]pyrimidine-2(1H)-thione (**7j**).* Yellow solid; mp 118–120 °C; IR (KBr) ν_{max}: 2923, 1517, 1055 cm^{-1}. Anal. calcd. for $C_{26}H_{28}Cl_4N_4OS$: C, 53.25; H, 4.81; N, 9.55. Found: C, 52.55; H, 4.27; N, 9.02. ^{1}H NMR (500 MHz, $CDCl_3$): δ_H 2.21–2.32 (m, 6H, CH_2-1′, CH_2-4′), 2.53–2.58 (m, 2H, CH_2-2′), 2.97 (d, J = 16.79 Hz, H-5a), 3.15 (d, J = 16.79 Hz, H-5b), 3.58 (d, J = 13.10 Hz, H-7a), 3.71–3.82 (m, 5H, H-7b, CH_2-5′), 5.73 (s, 1H, H-4), 6.88 (s, 1H, H-9), 7.11 (s, 1H, NH), 7.22-7.47 (m, 6H, H-aromatic), 7.83 (s, 1H, NH). ^{13}C NMR (125 MHz, $CDCl_3$): δ_C 52.58, 52.69, 53.46, 54.19, 55.27, 57.11, 66.89, 110.25, 122.17, 127.49, 127.87, 128.19, 129.43, 129.85, 130.32, 132.24, 132.45, 132.69, 133.19, 133.88, 134.07, 137.55, 174.48.

4.2. AChE and BChE inhibitory assays

Cholinesterase inhibitory activity of the synthesized compounds was evaluated using the Ellman's microplate assay following method described by Ahmed and Gilani [35]. For acetylcholinesterase (AChE) inhibitory assay, 140 μL of 0.1 M sodium phosphate buffer (pH 8) was first added to a 96-well microplate followed by 20 μL of test samples and 20 μL of 0.09 units/mL acetylcholinesterase enzyme from *Electrophorus electricus* (Sigma). After 15 min of incubation at 25 °C, 10 μL of 10 mM 5,5′-dithiobis-2-nitrobenzoic acid (DTNB) was added into each well followed by 10 μL of acetylthiocholine iodide (14 mM). At 30 min after the initiation of enzymatic reaction, absorbance of the colored end-product was measured using BioTek PowerWave X 340 Microplate Spectrophotometer at 412 nm. For butyrylcholinesterase (BChE) inhibitory assay, the same procedures were followed except for the use of enzyme and substrate, whereby butyrylcholinesterase from equine serum and *S*-butyrylthiocholine chloride (14 mM) were used, respectively.

Galantamine was used as positive control. Test samples and galantamine were prepared in DMSO at an initial concentration of 1 mg/mL (1000 ppm). The concentration of DMSO in final reaction mixture was 1%. At this concentration, DMSO has no inhibitory effect on both acetylcholinesterase and butyrylcholinesterase enzymes.

The initial screening was carried out at 10 μg/mL of test samples in 1% DMSO and each test was conducted in triplicates. Absorbencies of the test samples were corrected by subtracting the absorbance of their respective blank. Percentage enzyme inhibition is calculated using the following formula:

$$\text{Percentage of inhibition} = \frac{\text{Absorbance of control} - \text{Absorbance of sample}}{\text{Absorbance of control}} \times 100$$

Subsequently, the determination of IC_{50} was carried out using a set of five concentrations.

4.3. Molecular modeling

In order to investigate possible interactions between the synthesized compounds and the active site of acetylcholinesterase and butyrylcholinesterase, molecular docking study was performed. Using Glide, (version 5.7, Schrödinger, LLC, New York, NY, 2011), compounds **6a** and **7b** were docked onto the active site of *Tc*AChE derived from three-dimensional structure of the enzyme complex with anti-Alzheimer's drug, donepezil (PDB ID: 1EVE) and **7b** to BChE derived from complex of the enzyme with its substrate (PDB code: 1P0P).

Water molecules and hetero groups were deleted from receptor beyond the radius of 5 Å of reference ligand (donepezil or BCh), resulting protein structure refined and minimized by Protein Preparation Wizard using OPLS-2005 force field. Receptor Grid Generation program were used to prepare AChE and BChE grid and all the ligands were optimized by LigPrep program by using OPLS-2005 force field to generate lowest energy state of ligands. Docking stimulations were carried out on bioactive compounds resulting in 5 poses per ligand, in which the best pose with highest score was displayed for each ligand.

Acknowledgments

We would like to thank the Malaysian Government and Universiti Sains Malaysia (USM) for the Research University Grant (1001/PFARMASI/813031). AB is supported by the USM Graduate Assistant Scheme from the Institute for Postgraduate Studies (IPS) of Universiti Sains Malaysia.

Appendix A. Supplementary data

Supplementary data associated with this article can be found in the online version, at http://dx.doi.org/10.1016/j.ejmech.2013.06.054.

References

[1] N.L. Batsch, M.S. Mittleman, World Alzheimer's Report 2012, World Alzheimer's Soceity, 2012.
[2] J. Hardy, Alzheimer's disease: the amyloid cascade hypothesis: an update and reappraisal, J. Alzheimers Dis. 9 (2006) 151–153.
[3] C. Geula, M.M. Mesulam, Cholinesterases and the pathology of Alzheimer disease, Alzheimer Dis. Assoc. Disord. 9 (1995) 23–28.
[4] A. Martorana, Z. Esposito, G. Koch, Beyond the cholinergic hypothesis: do current drugs work in Alzheimer's disease? CNS Neurosci. Ther. 16 (2010) 235–245.

[5] M. Farlow, M. Miller, V. Pejovic, Treatment options in Alzheimer's disease: maximizing benefit, managing expectations, Dement. Geriatr. Cogn. Disord. 25 (2008) 408–422.
[6] G. Benzi, A. Moretti, Is there a rationale for the use of acetylcholinesterase inhibitors in the therapy of Alzheimer's disease? Eur. J. Pharm. Sci. 346 (1998) 1–13.
[7] N. Tabet, Acetylcholinesterase inhibitors for Alzheimer's disease: anti-inflammatories in acetylcholine clothing, Age Ageing 35 (2006) 336–338.
[8] E. Giacobini, Cholinesterase inhibitors: new roles and therapeutic alternatives, Pharmacol. Res. 50 (2004) 433.
[9] N. Greig, T. Utsuki, D. Ingram, Y. Wang, G. Pepeu, C. Scali, Q. Yu, J. Mamczarz, H. Holloway, T. Giordano, D. Chen, K. Furukawa, K. Sambamurti, A. Brossi, D. Lahiri, Selective butyrylcholinesterase inhibition elevates brain acetylcholine, augments learning and lowers Alzheimer β-amyloid peptide in rodent, Proc. Natl. Acad. Sci. U.S.A. 102 (2005) 17213–17218.
[10] W. Xie, J.A. Stribley, A. Chatonnet, P.J. Wilder, A. Rizzino, R.D. McComb, P. Taylor, S.H. Hinrichs, O. Lockridge, Postnatal developmental delay and supersensitivity to organophosphate in gene-targeted mice lacking acetylcholinesterase, J. Pharmacol. Exp. Ther. 293 (2000) 896–902.
[11] C. Holmes, C. Ballard, D. Lehmann, A. David Smith, H. Beaumont, I.N. Day, M. Nadeem Khan, S. Lovestone, M. McCulley, C.M. Morris, D.G. Munoz, K. O'Brien, C. Russ, T. Del Ser, D. Warden, Rate of progression of cognitive decline in Alzheimer's disease: effect of butyrylcholinesterase K gene variation, J. Neurol. Neurosurg. Psychiatry 76 (2005) 640–643.
[12] D.B. Kitchen, H. Decornez, J.R. Furr, J. Bajorath, Docking and scoring in virtual screening for drug discovery: methods and applications, Nat. Rev. Drug Discov. 3 (2004) 935–949.
[13] J.L. Sussman, M. Harel, F. Frolow, C. Oefner, A. Goldman, L. Toker, I. Silman, Atomic structure of acetylcholinesterase from Torpedo californica: a prototypic acetylcholine-binding protein, Science 253 (1991) 872–879.
[14] M. Harel, D.M. Quinn, H.K. Nair, I. Silman, J.L. Sussman, The X-ray structure of a transition state analog complex reveals the molecular origins of the catalytic power and substrate specificity of acetylcholinesterase, J. Am. Chem. Soc. 118 (1996) 2340–2346.
[15] M. Harel, I. Schalk, L. Ehret-Sabatier, F. Bouet, M. Goeldner, C. Hirth, P.H. Axelsen, I. Silman, J.L. Sussman, Quaternary ligand binding to aromatic residues in the active-site gorge of acetylcholinesterase, Proc. Natl. Acad. Sci. U.S.A 90 (1993) 9031–9035.
[16] L. Pezzementi, F. Nachon, A. Chatonnet, Evolution of acetylcholinesterase and butyrylcholinesterase in the vertebrates: an atypical butyrylcholinesterase from the Medaka *Oryzias latipes*, PLoS One 6 (2011) e17396.
[17] A.N. Çokuğraş, Butyrylcholinesterase: structure and physiological importance, Turk. J. Biochem. 28 (2003) 54–61.
[18] N. Isambert, M.M.S. Duque, J.C. Plaquevent, Y. Enisson, J. Rodriguez, T. Constantieux, Multicomponent reactions and ionic liquids: a perfect synergy for eco-compatible heterocyclic synthesis, Chem. Soc. Rev. 40 (2011) 1347–1357.
[19] M. Petkovic, K.R. Seddon, L.P.N. Rebelo, C.S. Pereira, Ionic liquids: a pathway to environmental acceptability, Chem. Soc. Rev. 40 (2011) 1383–1403.
[20] K.S. Atwal, G.C. Rovnyak, B.C. O'Reilly, J. Schwartz, Substituted 1,4-dihydropyrimidines. 3. Synthesis of selectively functionalized 2-hetero-1, 4-dihydropyrimidines, J. Org. Chem. 54 (1989) 5898–5907.
[21] G.C. Rovnyak, K.S. Atwal, A. Hedberg, S.D. Kimball, S. Moreland, J.Z. Gougoutas, B.C. O'Reilly, J. Schwartz, M.F. Malley, Dihydropyrimidine calcium channel blockers. 4. Basic 3-substituted-4-aryl-1,4-dihydropyrimidine-5-carboxylic acid esters. Potent antihypertensive agents, J. Med. Chem. 35 (1992) 3254–3263.
[22] D. Nagarathnam, S.W. Miao, B. Lagu, G. Chiu, J. Fang, T.G.M. Dhar, J. Zhang, S. Tyagarajan, M.R. Marzabadi, F. Zhang, Design and synthesis of novel α1a adrenoceptor-selective antagonists. 1. Structure–activity relationship in dihydropyrimidinones, J. Med. Chem. 42 (1999) 4764–4777.
[23] C.O. Kappe, Biologically active dihydropyrimidones of the Biginelli-type—a literature survey, Eur. J. Med. Chem. 35 (2000) 1043–1052.
[24] G.P. Black, S.J. Coles, A. Hizi, A.G. Howard-Jones, M.B. Hursthouse, A.T. McGown, S. Loya, C.G. Moore, P.J. Murphy, N.K. Smith, Synthesis and biological activity of analogues of ptilomycalin A, Tetrahedron Lett. 42 (2001) 3377–3381.
[25] T.U. Mayer, T.M. Kapoor, S.J. Haggarty, R.W. King, S.L. Schreiber, T.J. Mitchison, Small molecule inhibitor of mitotic spindle bipolarity identified in a phenotype-based screen, Science 286 (1999) 971–974.
[26] A.D.K. Patil, N.V. Kokke, W.C. Bean, Novel alkaloids from the sponge *Batzella* sp.: inhibitors of HIV gp120-human CD4 binding, J. Org. Chem. 60 (1995) 1182–1188.
[27] T. Mohamed, P.P. Rao, Design, synthesis and evaluation of 2,4-disubstituted pyrimidines as cholinesterase inhibitors, Bioorg. Med. Chem. Lett. 20 (2010) 3606–3609.
[28] T. Mohamed, X. Zhao, L.K. Habib, J. Yang, P.P. Rao, Design, synthesis and structure–activity relationship (SAR) studies of 2,4-disubstituted pyrimidine derivatives: dual activity as cholinesterase and Aβ-aggregation inhibitors, Bioorg. Med. Chem. 19 (2011) 2269–2281.
[29] T. Mohamed, J.C. Yeung, M.S. Vasefi, M.A. Beazely, P.P. Rao, Development and evaluation of multifunctional agents for potential treatment of Alzheimer's disease: application to a pyrimidine-2,4-diamine template, Bioorg. Med. Chem. Lett. 22 (2012) 4707–4712.
[30] A. Basiri, V. Murugaiyah, H. Osman, R.S. Kumar, Y. Kia, M.A. Ali, Microwave assisted synthesis, cholinesterase enzymes inhibitory activities and molecular docking studies of new pyridopyrimidine derivatives, Bioorg. Med. Chem. 21 (2013) 3022–3031.
[31] J. Figueiredo, M. Ismael, J. Pinheiro, A. Silva, J. Justino, F. Silva, M. Goulart, D. Mira, M. Araújo, R. Campoy, Facile synthesis of oxo-/thioxopyrimidines and tetrazoles C–C linked to sugars as novel non-toxic antioxidant acetylcholinesterase inhibitors, Carbohydr. Res. 347 (2012) 47–54.
[32] Crystallographic data (excluding structure factors) for pyridopyrimidine-2-thiones **7b** in this letter have been deposited with the Cambridge Crystallographic Data Centre as supplementary publication number CCDC 936212. Copies of the data can be obtained, free of charge, on application to CCDC, 12 Union Road, Cambridge CB2 1EZ, UK [fax: +44(0)1223–336033 or e-mail: deposit@ccdc.cam.ac.uk].
[33] J. Cheung, M.J. Rudolph, F. Burshteyn, M.S. Cassidy, E.N. Gary, J. Love, M.C. Franklin, J.J. Height, Structures of human acetylcholinesterase in complex with pharmacologically important ligands, J. Med. Chem. 55 (2012) 10286.
[34] Y. Nicolet, O. Lockridge, P. Masson, J.C. Fontecilla-Camps, F. Nachon, Crystal structure of human butyrylcholinesterase and of its complexes with substrate and products, J. Biol. Chem. 278 (2003) 41141–41147.
[35] T. Ahmed, A.H. Gilani, Inhibitory effect of curcuminoids on acetylcholinesterase activity and attenuation of scopolamine-induced amnesia may explain medicinal use of turmeric in Alzheimer's disease, Pharmacol. Biochem. Behav. 91 (2009) 554–559.